Surface analysis of human plasma fibronectin adsorbed to commercially pure titanium materials

D. E. MacDonald,[1,2,4] B. Markovic,[1] M. Allen,[3] P. Somasundaran,[1] A. L. Boskey[4]
[1]*Langmuir Center for Colloids & Interfaces, Columbia University, 911 S.W. Mudd Building, Mail Code 4711, 500 West 120th Street, New York, New York 10027*
[2]*V.A. Medical Center, Bronx, New York*
[3]*Digital Instruments, Santa Barbara, California*
[4]*Hospital for Special Surgery, New York, New York*

Received 2 June 1997; accepted 5 November 1997

Abstract: Protein binding on metallic implant surfaces, such as titanium, is governed by the physico–chemical nature of the metallic surface. Human plasma fibronectin (HPF) is an important matrix glycoprotein that mediates cell and protein attachment to each other or to the extracellular matrix present during wound healing. The objective of this study was to investigate the adsorption of HPF onto polished commercially pure titanium (cpTi) by using atomic force microscopy (AFM) and electron spectroscopy for chemical analysis (ESCA) and to measure the resultant surface contact angle before and after HPF binding. Two types of cpTi disks, one highly polished in our laboratory (HSS) and one commercially prepared (3I), were reacted with HPF solutions of varying concentrations (1 μg/mL—10 ng/mL). ESCA survey spectra of samples coated with 1 μg/mL of fibronectin showed an increase in organic nitrogen and carbon compared with uncoated controls. Contact angle measurements of HSS and 3I cpTi disks showed no significant difference in average contact angle (36.3° ± 3.5 and 39.1° ± 3.1) despite differences in local root mean square (RMS) surface roughness (4.45 ± 0.46 nm and 22.37 ± 4.17 nm) as measured by AFM. Images obtained by AFM showed that 3I specimens were more irregular, with large parallel polishing grooves. Adsorbed HPF appeared in a globular form with an average length of 16.5 ± 1.0 nm, a height of 2.5 ± 0.5 nm, and a width of 9.6 ± 1.2 nm. Fibronectin coating on both HSS and 3I cpTi specimens resulted in a significant increase in hydrophobicity compared to uncoated specimens. These results indicate the significance of HPF on cpTi and may explain how cpTi implants function *in situ*. © 1998 John Wiley & Sons, Inc. J Biomed Mater Res, 41, 120–130, 1998.

Key words: implant surface; titanium; fibronectin; atomic force microscopy; contact angle

INTRODUCTION

Upon implantation, the surfaces of synthetic materials invariably become coated with a thin proteinacious film.[1] Protein orientation will be dependent on the particular binding surface, and various surface characteristics may modify their biologic activity in relation to cell attachment.[2] Titanium, a biocompatible metal commonly used in medical implants, is known to form an oxide layer,[3] and the interaction of cells with this layer is mediated by the extracellular matrix proteins produced by the cell as well as by cell surface proteins. It is critical to have as much accurate information on the characteristics of the metal surfaces as possible, and it is the aim of this paper to examine such characteristics using advanced surface-probe techniques.

Fibronectin, one of the earliest cell-binding proteins produced by odontoblasts and osteoblasts,[4–7] is believed to play an important role in governing the interactions of implants with their surrounding matrix. Fibronectin is a high molecular weight glycoprotein (MW = 440,000 daltons) that is involved in cell adhesion and is located in body fluid, connective tissue, and basement membranes.[8] It is composed of two dimeric chains, each 60 nm in length and 2.5 nm in diameter, connected by flexible disulfide bonds near one end of each chain, and it is known to bind to a number of substrates and assume different conformations during such binding.[9–13] UV fluorescence microscopic studies have suggested that fibronectin protein binding involves the interaction of charged groups at the surface of the molecule.[14]

Correspondence to: D. MacDonald
Contract grant sponsor: National Institutes of Health; Contract grant number: DE04141
Contract grant sponsor: National Science Foundation; Contract grant number: CTS-9622781

 CCC 0021-9304/98/010120-11

The adsorption of fibronectin onto different substrates has been investigated by a number of different methods. Emch and coworkers have imaged fibronectin with scanning tunneling microscopy (STM) on mica shadowed with a thin platinum carbide-conductive film.[15] Using scanning force microscopy (SFM) of fibronectin sprayed on mica and polymethylmethacrylate (PMMA), protein morphology was found to be influenced by substrate surface properties.[16] The application of this information to *in vivo* situations was limited because of the nonaqeous environment used for analysis.

Atomic force microscopy (AFM) is known to provide topographical images at the fluid–solid interface.[17,18] Its ability to view surface topography in a liquid medium, unaltered through sample preparation of tip interaction during the scanning process, makes it a valuable analytical tool. For this reason, AFM was used in this study to investigate the adsorption of fibronectin onto polished commercially pure (cp) titanium surfaces along with electron spectroscopy for chemical analysis (ESCA) and contact angle measurements for characterizing the titanium substrate.

MATERIALS AND METHODS

Surface preparation

Two sets of implant specimens were prepared and analyzed, one set custom prepared at the Hospital for Special Surgery (HSS) and another obtained commercially from 3I Implant Innovations, West Palm Beach, FL.

The titanium disks (12 mm in diameter) prepared at HSS were from a 1.5 mm thick, commercially pure titanium (cpTi) sheet (President Titanium, Hanson, MA). The disks were wet-ground with 320 through 400 grit silicon carbide paper (smooth samples), deburred, and further polished with 85FNEXL and 7S Scotch Brite nonwoven nylon mesh wheels (3M, Indianapolis, IN) and then with coarse and fine Aluminum oxide compound (Matchless Metal Polish Company, Chicago, IL) on clean Grade NWY 86/87 buff wheels (Divine Brothers Co., Utica, NY). The specimens were rinsed with distilled water at each step. The metallic samples were precleaned ultrasonically in Alkanox followed by a wash cycle in a Chemcrest 200 cleaning console unit (Crest Ultrasonic Corp., Trenton, NJ) at 66°C and spray washed twice in distilled water. Other cpTitanium disks (rough surface) were provided by 3I Implant Innovations (West Palm Beach, FL) and prepared according to the manufacturer's specifications.

To ensure cleanliness of all the specimens, the disks (both the specially fabricated and the commercial) were washed successively in isopropanol, acetone, xylene, acetone, and 1M ammonium hydroxide, and, finally, with deionized water. The samples then were passivated in 40% nitric acid and rinsed three times with deionized water, dried, and stored covered under a UV light in a cell culture hood (Forma Scientific, Marietta, OH). The Ti disks with and without fibronectin then were evaluated by means of ESCA, contact angle, and atomic force microscopy (AFM).

Fibronectin

Affinity-purified human plasma fibronectin was obtained from Calbiochem (LaJolla, CA). A buffer solution (TBS) containing 0.05*M* Tris and 0.15*M* NaCl, pH 7.4, was prepared and sterilized by filtration through a 0.22 micron Falcon Easy Flow™ filter (Becton Dickinson, Lincoln Park, NJ) under vacuum. Human plasma fibronectin solutions of 1 μg/mL, 100 ng/mL, 10 ng/mL, and 1 ng/mL were prepared in this TBS buffer. The cpTi disks then were placed in 1 mL of each of these solutions in 13 mL polypropylene tubes (Sarstedt, Newton, NC) and allowed to incubate for 1 h at 37°C with gentle orbital shaking. Control specimens were placed in TBS buffer alone. The samples then were left in solution and stored at −70°C until ready for analysis.

Surface analysis

Electron spectroscopy for chemical analysis (ESCA) of the untreated and fibronectin (1 μg/mL) precoated surfaces was conducted using a Physical Electronics (PHI) model 5600 ESCA spectrometer (Eden Prairie, MN). Titanium samples (uncoated and coated by fibronectin) were allowed to reach room temperature in covered containers, carefully rinsed with deionized water, dried at room temperature, and then analyzed. A monchromatic X-ray source equipped with an aluminum anode (AlKα = 1486.6 eV) operated at 400 W in the diffuse mode was used to excite photoemission. Emitted photoelectrons were analyzed using a spherical capacitor electron energy analyzer with an Omni Focus III small area lens. The analyzer was operated in the fixed analyzer transmission mode. The angle between the plane of the sample and analyzer lens was 65° for all analyses. ESCA survey spectra were obtained using an analyzer pass energy of 188 eV while high resolution multiplex data of the titanium implant disks were obtained at a pass energy of 29 eV. An analysis area of 800 μm was used for characterization of the titanium implant surfaces. An electron flood gun operated at 20 mA emission current and 10 eV electron energy was used to neutralize sample charging during analysis. The residual vacuum inside the spectrometer was 3.1×10^{-9} Torr or lower during analysis. Data acquisition and storage was accomplished using an HP Apollo 425 work station running PHI-Access software. The atomic percentages of the elements present on the titanium surfaces were calculated using software and atomic sensitivity factors included with the instrument data system. The binding energies of the photoelectron peaks were referenced to the C 1s line at 284.6 eV.

Contact angle determination

Contact angle analysis was performed on metallic surfaces prior to and after fibronectin binding. Drops of distilled wa-

ter were placed on the specimens and contact angles measured using a NRL-100 contact angle goniometer automated with image analysis software (Rame–Hart, Mountain Lakes, NJ). A total of 15 HSS and 15 3I specimens for control and coated surfaces was analyzed. Eight timed measurements over a 15 s interval were made for each surface type, and all analyses were performed at the same temperature and humidity.

Atomic force microscopy

Titanium samples slowly were defrosted to room temperature, carefully handled at the disk edges, and rinsed with an indirect flow of several milliliters of ultrapure distilled water. Any excess fluid then was wicked off the sides of the disks using tissue adsorbent paper, and the samples immediately were loaded into the AFM (Digital Instruments, Santa Barbara, CA). The samples were analyzed at room temperature and humidity. The MultiMode AFM and NanoScope IIIa controller equipped with an Extender Electronics Module for phase-lag detection were used for the analysis.

In order to reduce the possibility of smearing the protein molecules on the metallic surface, AFM was performed in a Tapping Mode™. A 125 μm long, single-arm silicon cantilever with end-mounted probe tips 5–10 nm in radius of curvature (TESP probes) were oscillated at cantilever resonance (300 kHz) with the initial amplitude corresponding to 1.25 volts. The initial amplitude setpoint was decreased by approximately 30% following engagement to allow good probe tip tracking of the sample surface. The integral and proportional gains typically were set to 0.4 and 0.6, respectively. Scanning frequencies of 0.3–3 Hz were used.

To visualize the underlying cpTitanium surface after the application of a fibronectin coating, an AFM probe tip was used to carefully "scrape" off the proteinacious layer, creating a window-like effect. A 450 μm long, single-arm silicon cantilever with end-mounted probe tips 5–10 nm in radius of curvature (ESP probes) were used. During probe-tip engagement on the sample, cantilever deflection resulted in a 1.0 volt change in the vertical difference signal for the photodetector. For imaging, the "setpoint" then was decreased to −1.0 volt to minimize the probe-tip force on the sample. For "scraping" experiments, the "setpoint" temporarily was increased to 5–10 volts. Integral and proportional gains typically were set to 6 and 8, respectively. Scanning frequencies of 2–10 Hz were used. Scan rotation was 0 degrees for all imaging, with the scan direction parallel to the long axis of the cantilever.

Surface roughness determination

Quantitative measurements of the local root mean square (RMS) surface roughness were determined using both 3 μm × 2 μm and 500 nm × 500 nm AFM scans. The RMS roughness is defined as the height fluctuations in a given area. RMS roughness measurements were made in five random areas per uncoated specimen and computed with a roughness analysis program (Digital Instruments, Santa Barbara, CA).

Statistical analysis

The contact angle data were summarized and analyzed using a two-way analysis of variance (ANOVA) for both surfaces, coated or not, and for both HSS and 3I specimens. The alpha level was set at the 0.01 level.

RESULTS

ESCA surface analysis

HSS disks

Carbon, oxygen, titanium, nitrogen and aluminum were detected on the surface of the HSS prepared cpTi disks [Fig. 1(a), Table I]. The carbon concentration was less than that for the commercially prepared disk (3I), indicating that less organic material is present on the surface. The carbon species detected were similar to those found on the commercial disk. Nitrogen was present in two chemical forms: organic nitrogen (76%) and N^+ (24%). Titanium was present primarily as TiO_2, with less than 5% titanium metal, suggesting that the disk was covered with a TiO_2 layer. Aluminum was present on the disk as Al^{3+}, predominantly as Al_2O_3.

3I disks

Carbon, oxygen, nitrogen, and titanium were detected on the surface [Fig. 1(c), Table I]. Carbon was present in several forms, primarily as CH_x, hydrocarbon. Carbon also was present in functional groups having carbon–nitrogen or carbon–oxygen bonds. Nitrogen was present in two chemical forms, as organic nitrogen (amine or amide) and as singly charged nitrogen, N^+. Approximately 12% of the total nitrogen was present as N^+. Titanium was present almost entirely as TiO_2. Less than 5% of the total titanium was metallic Ti, which would further suggest that the titanium disk is covered with a TiO_2 layer.

ESCA survey spectra obtained of cpTitanium coated with 1 μg/mL fibronectin [Fig. 1(b,d), Table I] showed an increase in organic nitrogen and carbon when compared with uncoated controls. High resolution spectra of the C_{1s} and N_{1s} regions (Fig. 2) also showed the increased presence of characteristic protein functional groups (C-N, C-O, N-C=O).

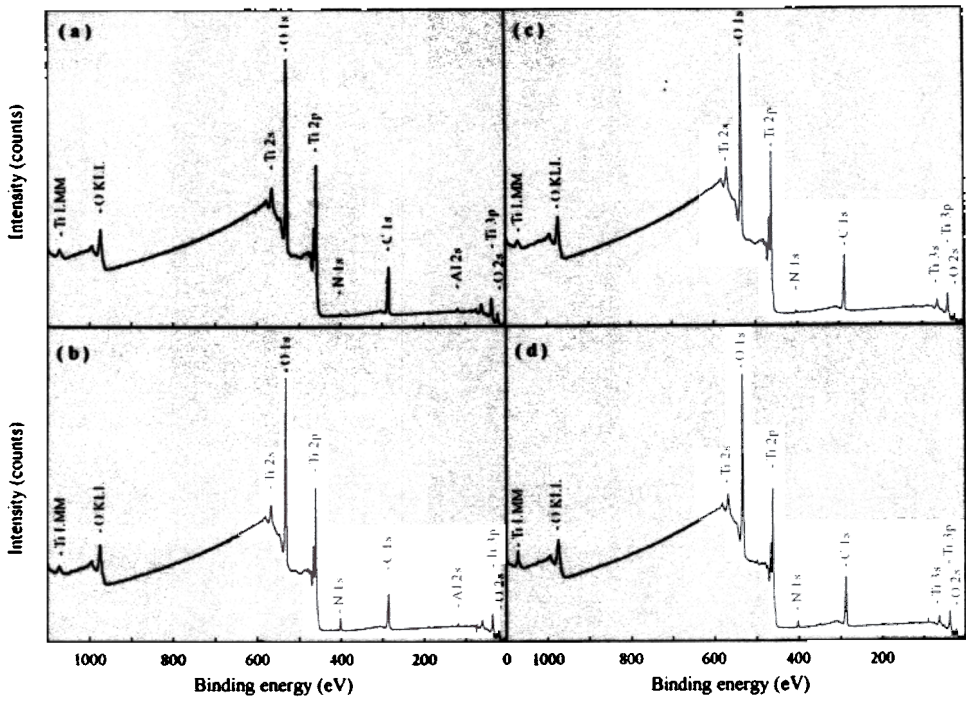

Figure 1. ESCA survey spectra of: (a) HSS prepared cp titanium sample; (b) HSS prepared cp titanium sample coated with fibronectin at a concentration of 1 μg/mL; (c) commercial 3I titanium sample; (d) commercial 3I titanium sample coated with fibronectin at a concentration of 1 μg/mL.

Contact angle measurements

Contact angle measurements of the control HSS and 3I cpTi disks showed an average contact angle of 36.3 ± 3.5 and 39.1 ± 3.1, respectively (Table II). No difference was noted between the receding and advancing contact angles of either of the control specimens. A comparison of contact angle measurements made between native and coated titanium specimens demonstrated that the presence of a protein coating resulted in a more hydrophobic surface ($P < 0.001$, Table II). No difference in contact angle measurements could be detected in the range of 1 μg/mL and 10 ng/mL fibronectin concentrations for coating ($P = 0.2$).

TABLE I
ESCA Results for HSS Prepared and Commercial 3I Titanium Samples Uncoated and Coated With Human Plasma Fibronectin

HSS Prepared cpTi Sample		Fibronectin-Coated HSS Prepared cpTi Sample	
Element	Concentration (%)	Element	Concentration (%)
C_{1s}	19.90	C_{1s}	25.54
O_{1s}	54.35	O_{1s}	49.54
Ti_{2p}	20.76	Ti_{2p}	17.64
N_{1s}	1.76	N_{1s}	4.34
Al_{2p}	3.23	Al_{2p}	2.78
3I cpTi Sample		**Fibronectin-Coated 3I cpTi Sample**	
Element	Concentration (%)	Element	Concentration (%)
C_{1s}	23.99	C_{1s}	31.83
O_{1s}	53.17	O_{1s}	48.05
Ti_{2p}	21.13	Ti_{2p}	17.45
N_{1s}	1.40	N_{1s}	2.67

Atomic force microscopy

In AFM, polished surfaces of HSS disks demonstrated areas of polishing grooves with small regions of surface pitting [Fig. 3(a)]. Commercially prepared 3I specimens showed a more irregular topography [Fig. 3(b)] with large parallel grooves.

When the same surfaces were exposed to 10 ng/mL of human plasma fibronectin in a buffered TBS solution, the surfaces appeared coated by many small compact protein clusters [Fig. 3(d)]. The control specimens were void of any protein material [Fig. 3(c)]. The protein clusters did not appear to show a preference for areas containing polishing grooves and were evenly dispersed on the HSS-prepared samples. On the commercially prepared 3I specimens, the protein appeared to aggregate within the deeper surface-finishing grooves. At a higher magnification with a scanned area of 74.4 nm, the fibronectin molecule appeared in globular form, with an average length of 16.5 ± 1.0 nm [Fig. 3(e)]. The average height of ten separate molecules was measured to be 2.5 ± 0.5 nm,

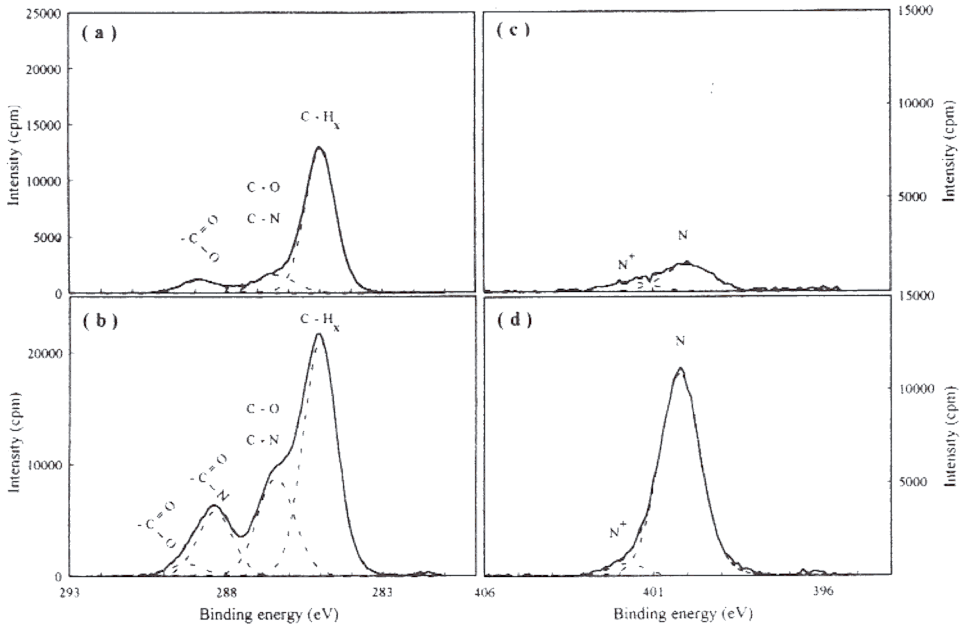

Figure 2. High resolution ESCA spectra of HSS cp titanium sample uncoated (a and c) and coated (b and d) with fibronectin. C_{1s} and N_{1s} regions are presented.

and the width measured was 9.6 ± 1.2 nm. Quantification of protein size was not possible on the 3I specimens due to the irregular nature of the surface.

By increasing the concentration of fibronectin to 1 μg/mL, a mat-like surface coating was observed with AFM [Fig. 3(f)] on the HSS specimen. When the AFM stylus purposely was pulled across the coating, the crosslinked fibronectin layer rolled back upon itself, revealing the underlying metallic surface [Fig. 3(g)].

Surface roughness determination

The RMS roughness measurement for commercially prepared 3I disks was 22.37 nm ± 4.17 at a scanned area of 3 μm × 2 μm and 12.23 nm ± 3.42 when scanned at 500 nm × 500 nm. Extensively finished surfaces prepared at HSS were considerably smoother with RMS values of 4.45 nm ± 0.46 at a scanned area of 3 μm × 2 μm and 3.87 nm ± 2.6 at a scanned area of 500 nm × 500 nm. The 3I specimens revealed numerous scratch marks from wet grinding with a corresponding increase in RMS scores in comparison with HSS prepared disks.

TABLE II
Measurements of Water Contact Angle for HSS and 3I Titanium Samples Uncoated and Coated with Human Plasma Fibronectin

Sample	Contact Angle (°)
Commercial Ti	39.1 ± 3.1
Commercial Ti + HFN (10 ng/mL)	53.3 ± 4.7*
Commercial Ti + HFN (1 μg/mL)	55.9 ± 3.0*
HSS Ti	36.3 ± 3.5
HSS Ti + HFN (10 ng/mL)	54.4 ± 2.0*
HSS Ti + HFN (1 μg/mL)	53.0 ± 6.5*

Measurements are mean ± standard deviation. *Statistically significant at $P \leq 0.01$.

DISCUSSION

The excellent biocompatibility of titanium implants is due to the favorable titanium oxide–tissue interaction that occurs *in vivo*. An important protein involved in cell binding is fibronectin. Plasma fibronectin, a glycoprotein present in blood, has been shown to promote cell adhesion, wound healing, and embryonic development.[19] In this study, the appearance of fibronectin binding onto cp Titanium surfaces of different characteristics was visualized using tapping mode atomic force microscopy.

The ESCA survey spectrum of both HSS and 3I prepared cpTi disks demonstrated the presence of C, N, O, and Ti [Fig. 1(a,c)]. Higher resolution of the $Ti2_p$ spectrum for both control specimens identified three peaks whose positions and shapes were consistent for TiO_2 as reported in the literature.[3,20–22] The ESCA spectra of samples immersed in a fibronectin solution of different concentrations showed increased carbon and nitrogen signals characteristic of protein deposition [Fig. 1(b,d)].[23,24] Nitrogen was present in two forms: organic nitrogen and singlet N^+. This charged moiety is probably contributed by amino acids within the protein under the particular condition of the

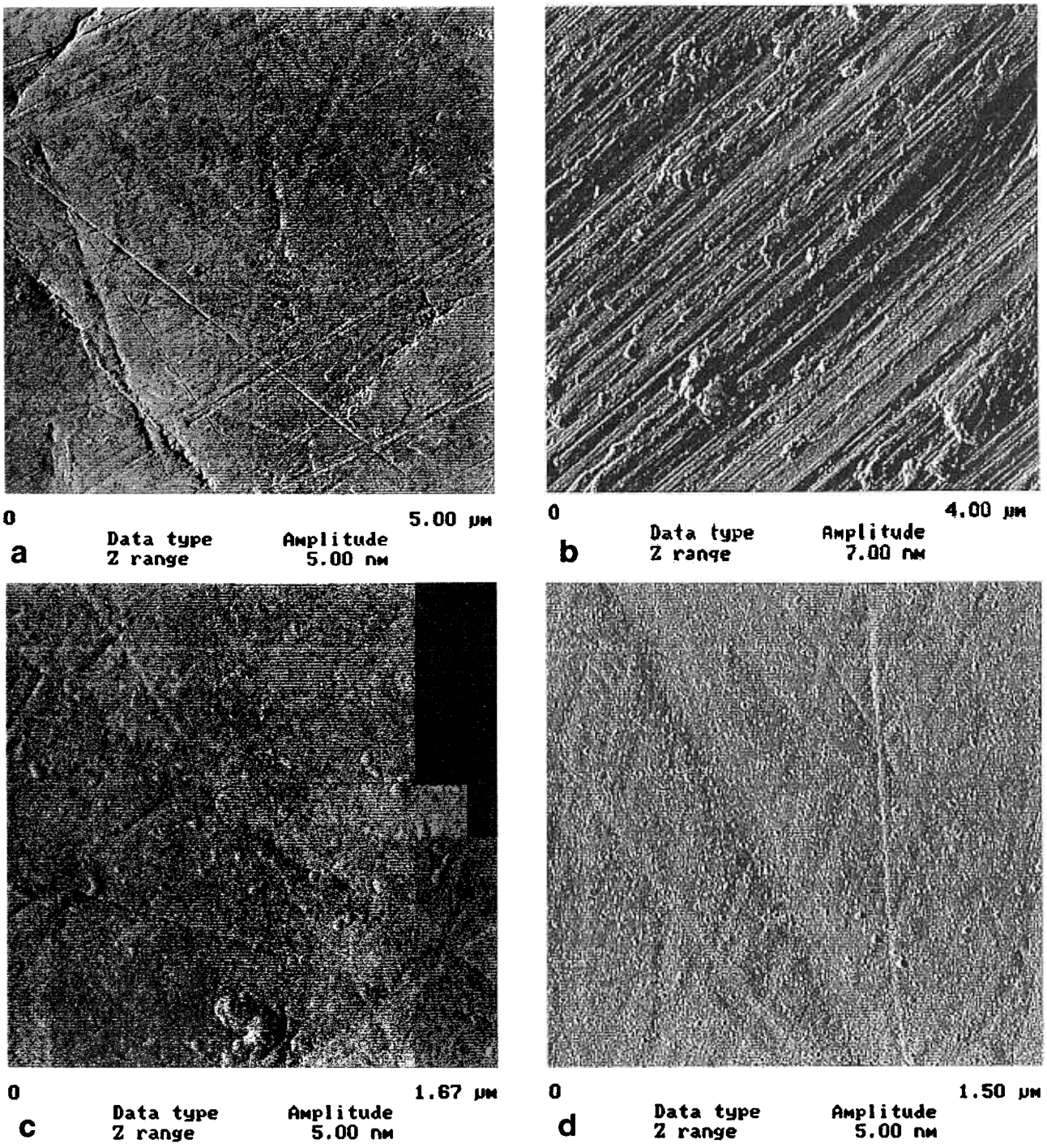

Figure 3. Atomic force microscopy (AFM) of cp titanium samples uncoated and coated by human plasma fibronectin: (a) Tapping Mode™ AFM image of HSS prepared cp titanium sample (scan size = 5 μm); (b) Tapping Mode™ AFM image of 3I prepared cp titanium sample (scan size = 4 μm); (c) Tapping Mode™ AFM image of HSS prepared cp titanium sample (scan size = 1.67 μm); (d) Tapping Mode™ AFM image of HSS prepared cp titanium sample coated with human plasma fibronectin at concentration of 10 ng/mL (scan size = 1.5 μm); (e) High resolution Tapping Mode™ AFM image showing globular form of human plasma fibronectin on HSS prepared cp titanium sample. Amplitude (left) and phase (right) mode (scan size = 74.4 nm); (f) Contact mode AFM image of HSS prepared cp titanium sample preincubated with 1 μg/mL of human plasma fibronectin before intentionally raised force scraping of protein layer. (deflection mode, scan size = 4.13 μm); (g) Contact mode AFM image of the same area in Figure 3(f) showing the rolled mat-like fibronectin surface coating exposing the metallic undersurface on HSS prepared cp titanium sample (deflection mode, scan size = 4.13 μm).

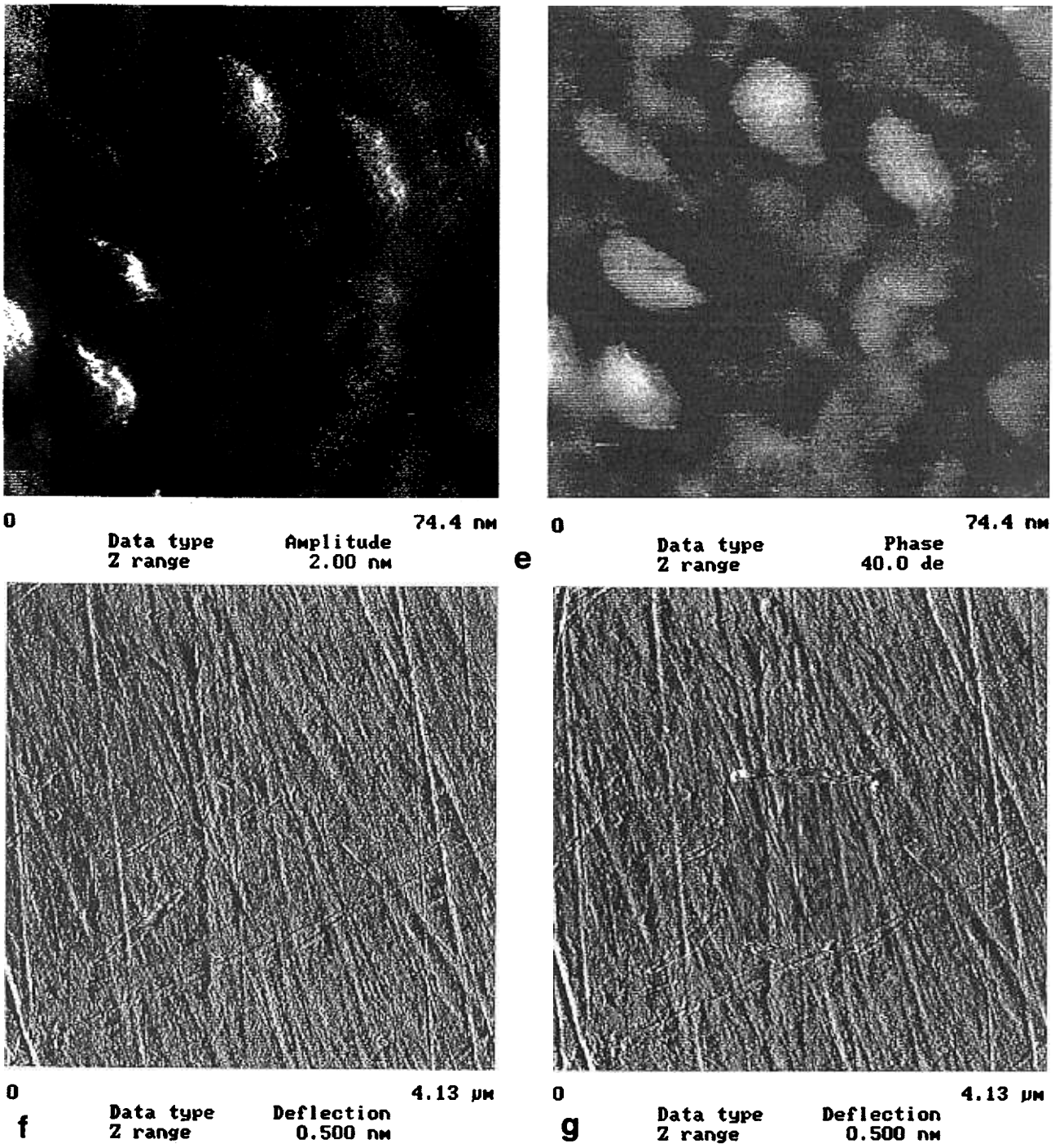

Figure 3. Continued.

analysis. The carbon species detected on the fibronectin-treated disks also were consistent with the presence of protein as C-N, C-O, and N-C=O functionalities were observed (Fig. 2). Slight amounts of polishing residue might account for the aluminum signal observed. A comparison of the titanium signal between control and coated specimens showed a reduction for the latter. This is best explained by the depth the beam penetrates. Because only the top 10 nm of the surface of each specimen is analyzed, the presence of a proteinacious coating would reduce the titanium signal due to the increased thickness the beam has to penetrate. The observed reduction in oxygen signal could be for a similar reason.

The wettability of any biological material depends on the magnitude of intermolecular forces present at the solid and liquid interface, expressed here in terms of contact angle Θ.[25] Wettability of particles appears to be surface roughness dependent. With increasing surface roughness the receding angle decreases and the

advancing angle increases.[26] It has been reported in the past that totally hydrophobic materials can be converted to hydrophilic ones by roughening their surfaces.[26–28] A comparison of contact angle measurements on sterilized polished and unpolished cpTi-coined flats showed larger contact angles for the unpolished sterilized specimens.[29] Although the contact angles on the rougher commercially prepared 3I specimens were larger when compared with the polished HSS prepared group, the difference was not statistically significant ($P > 0.05$). This is in agreement with reports that mechanically polishing or buff polishing metals has little effect on contact angle.[29–31] Some degree of surface roughness will result from mechanical polishing, and it is possible that the magnitude of roughness determines the overall contact angle. Our results, along with this, suggest that surface roughness will contribute to the wettability of a surface, yet a more important factor may be changes in surface chemical composition due to various environmental interactions and surface oxidation states.

As confirmed by the ESCA results, titanium and its alloys are covered mainly with TiO_2.[21,22,25,30,31] This phase determines both the contact angle and spreading behavior of a liquid drop on the surface.[30] Moreover, the process of passivation will affect the surface oxide layer.[32] Although at elevated temperatures these oxide layers undergo phase changes,[33] at the temperatures used for sterilization (autoclave, dry heat, UV) there appears to be no effect on contact angle measurements for cpTi.[29,34] However, the contact angles measured are lower than those reported in the literature.[30,34] The differences in surface treatment used in these studies account for the variations noted in contact angle between our specimens and those in the literature. This suggests that passivation, surface treatment, and temperature are important factors in determining the wettability of biological materials.[29]

Surface roughness is another variable. The AFM images of the commercially obtained 3I specimens and HSS samples showed a consistently more scratched surface on the former [Fig. 3(a,b)]. The RMS roughness measurements also were greater for the 3I specimens. Both the size of the scan and the area evaluated played a role in the RMS roughness measurements. With both samples analyzed, the RMS roughness scores increased with larger areas scanned. A possible explanation is that greater scanned areas can visualize surface features that might be overlooked on smaller scannings.[35]

At higher magnifications with a scanned area of 74.4 nm, the fibronectin molecule appeared in the globular form with an average length of 16.5 ± 1.0 nm [Fig. 3(e)]. This is comparable with the structure described by Koteliansky and coworkers[36] based on electron microscopic observation of fibronectin shadowed with tungsten–tantalum. They reported fibronectin globules with an average length of 15.5 ± 1.3 nm in length.[36,37] In contrast, rotary shadowing of fibronectin on mica has revealed lengths of 60 ± 7 nm to a range of 120 to 160 nm.[38,39] This variability of fibronectin chain length has been attributed to the extreme flexibility of the protein.[39] Fibronectin has been reported to have globular and filamentous forms depending on substrate and solution conditions.[40] The globular form of a particle may represent collapsed fibronectin molecules, which is the form found in solution.[41] In our study, the average height of ten separate molecules was measured to be 2.5 ± 0.5 nm, which is in accord with the reported value of 2.0 nm for the diameter of the fibronectin molecule based on electron microscopic analysis on mica.[39]

The conformation of the HPF molecule will vary depending on whether or not the molecule is in solution or is surface bound. Moreover, factors such as temperature, pH, and ionic strength of the local environment also will play a role in determining the molecular shape of fibronectin. In solution under normal physiologic conditions, fibronectin has been reported to assume a globular or compact form.[42,43] This compact form of fibronectin is stabilized by interdomain electrostatic interactions.[44] At temperatures above 40°C, extreme pH levels, or increased ionic strength, fibronectin assumes a more extended form.[44–48] Fibronectin is extremely flexible, and this extension due to local environmental changes does not result from denaturation of the molecule.[46] Based on the above considerations, it can be assumed that our experimental conditions of pH 7.4 and a temperature of 37°C would favor plasma fibronectin in a globular-like conformation when in solution. Unfortunately, little is known about the effect of these two factors on the structural nature of this protein molecule once it is adsorbed on a substrate. As indicated above, aside from temperature and pH, fibronectin conformation also may be ionic strength dependent, with the molecule being a compact form in a low salt environment and in an extended form in a high salt environment.[49] This interpretation has been questioned based on fluorescence energy studies which, in high salt solutions, describes a fibronectin molecule in which both the amino and carboxyl termini are juxtaposed whereas the central regions expand, creating a "balloon-like" effect.[50]

The conformation of fibronectin changes when it is adsorbed on a variety of surfaces. Erickson and Carrell reported that at high ionic strength (0.2*M* NaCl), fibronectin appeared as an extended molecule when visualized by sedimentation analysis on a mica surface.[51] At low ionic strengths (0.02*M* NaCl), fibronectin assumed a more compact structure. Half molecules and proteolytic fragments of fibronectin missing the terminal NH_2 or COOH groups underwent ionic strength-dependent changes in conformation similar to unaltered molecules. These conformational changes

were attributed to short range electrostatic interactions along the strand rather than to attraction of distant molecular segments.[51] In our investigation, use of a 0.15*M* salt solution did not result in the extended strands observed by Erickson and Carrell on mica.[51] This could be due to the different substrate, namely cpTi, and its effect upon protein conformation. Under similar salt and buffer conditions as in our study, Koteliansky and coworkers[36,37] observed the fibronectin to assume a compact protein structure. At the same initial salt concentration as that of our experiment, Wolff and Lai[50] reported some separation between the amino termini of plasma fibronectin immobilized onto Cytodex dextran beads, suggesting that some conformational changes may occur in the binding process. A possible explanation for the difference in appearance (folded versus unfolded) could be due to the different substrates used and the geometry of the substrate: beads versus smooth polished surfaces. Total internal reflection fluorescence (TIRF) of the local tryptophan microenvironment when plasma fibronectin was adsorbed to hydrophobic silica surfaces show the tryptophan groups shift into a more hydrophilic microenvironment.[52] Such a shift was not observed when the protein was tested on hydrophilic silica surfaces. Fluorescence energy transfer methods have been employed to estimate changes in intramolecular distance between plasma fibronectin chains before and after adsorption to hydrophilic Cytodex beads.[47,52] The energy transfer of fluorescein-labeled amino terminus groups and coumarin-labeled sulfhydryl groups was completely reduced, suggesting that interchain separation occurs after protein absorption. It should be noted that there was a high signal-to-noise ratio, which would indicate that the protein was not completely extended and that some variability in the results exists. Of the two protein chain sulfhydryl groups, one (SH-1) becomes exposed while the other (SH-2) remains buried when plasma fibronectin binds to polystyrene beads.[53,54] It is clear that there are a number of variables that dictate the conformation fibronectin may assume upon substrate binding. These conformational changes indeed can be expected to influence further the protein's exposed potential binding sites.

Scanning force micrographs of fibronectin adsorbed on hydrophilic (mica) and hydrophobic (polymethylmethacrylate) surfaces have shown that fibronectin shape is substrate dependent.[16] On the hydrophilic mica surfaces, fibronectin exhibited a V-shaped orientation whereas when sprayed on a hydrophobic PMMA surface, the protein formed a thin, dense meshwork over the surface. A consistent problem noted with SFM using traditional contact scanning was the destruction caused by the tip-surface interaction during the scanning process and destruction of the protein surface coating at higher resolution settings.[16] Moreover, in this work by Emch and coworkers,[16] all the extended fibronectin proteins appear to be oriented in the same direction. If protein binding is arbitrary and random, it would be difficult for all the proteins to assume the same "V" shape and same directional orientation. Possibly the force with which the sprayed protein contacts the surface may be sufficient to overcome some of the short range electrostatic interactions of the protein strand, creating an illusion of protein unfolding. Fibronectin in our study was allowed to react with the surface from a suspension, and no attempt was made to vigorously shake the reaction vessel nor to spray the metal surfaces with the protein to encourage binding. Therefore, the physical manipulation of the protein is proposed to have an effect on the shape it assumes on a surface.

Emch and coworkers[16] employed a volatile buffer in place of salt buffers since, if allowed to dry, precipitated salt crystals would obscure the resolution of the smaller fibronectin molecule. On titanium, we found this not to be the case provided the samples were kept moist throughout the procedure and carefully were rinsed several times with triple distilled water prior to analysis. This procedure would result in a lower ionic strength at the metallic–water interface. Samples were air dried to 50% relative humidity, thus leaving a water layer on the surface. Therefore, there was no exposure of the bound fibronectin to a high salt environment nor was there complete drying of the buffer containing the protein. Our findings suggest that the local ionic strength at the metallic–water interface during specimen preparation might be significant enough to affect the resultant protein conformation, whether globular or extended.

Upon increasing the concentration of fibronectin to 1 μg/mL, a mat-like surface coating was observed with AFM [Fig. 3(f)]. When the AFM stylus purposely was pulled across the coating, the crosslinked fibronectin layer could roll back upon itself revealing the underlying metallic surface [Fig. 3(g)]. These results support earlier observations that fibronectin has the capacity to form an interdigitating protein layer.[55] Once fibronectin–fibronectin crosslinking resulting in a fibrillar state in solution occurs, this complex demonstrates characteristics of an insoluble monolayer.[56] Thus, conformational changes appear to be necessary for the conversion of the soluble form of fibronectin to an insoluble form. Self assembly of fibronectin is central in the formation of the extracellular matrix. Several modules (I_1-I_2) located at the amino terminal end of each fibronectin arm are required for matrix assembly by fibroblasts and exhibit fibronectin–fibronectin binding properties.[57–60] Other segments (module III) are buried in intact insoluble fibronectin and become active only after surface binding.[59,60] Matrix assembly *in vivo* requires disulfide exchange in which two disulfide bonds of neighboring fibronectin molecules ex-

change with their binding partners.[61,62] This disulfide-bonded dimer structure is critical for fibronectin fibril formation.[59] Fibronectin molecules therefore can be proposed to line up with one another in such a manner as to optimize disulfide crosslinking.[56] This may enhance the interaction with the titanium surface.

CONCLUSIONS

Our results for fibronectin interaction with commercially pure titanium show the fibronectin protein to have a small globular structure of 16.5 ± 1.0 nm in length, 2.5 ± 0.5 nm in height, and 9.6 ± 1.2 nm in overall diameter when bound to a cpTitanium surface. The average contact angles for cpTi control specimens were 36.3 ± 3.5 and 39.1 ± 3.1 for the HSS and commercially prepared 3I specimens, respectively. In the presence of fibronectin, the surface appears more hydrophobic due to exposed moieties. Both survey and high resolution ESCA spectra have shown the presence of surface groups that are characteristic for adsorbed protein molecules. At higher concentrations, fibronectin appears to form a thin crosslinked matrix that can be lifted off the surface. It is important to note the implications of these conformational changes on the interaction with tissue cells. Future studies should focus on the effect of these interactions.

Generous support was received from a Physicians Career Development Award, V. A. Central Office, during the preparation of this article and for the studies described herein. Special thanks goes to Dr. Michael Stranick (Colgate Palmolive Company, Piscataway, NJ) for the ESCA analysis and to Kelly O'Hara (Rame-Hart, Inc., Mountain Lakes, NJ) for use of the NRL-100-00-S automatic contact angle goniometer. Thanks also go to Dr. Timothy Wright, Hospital for Special Surgery (NY, NY) for preparation of the polished cpTitanium specimens and to Dr. Richard Caudill of the 3I Implant Innovations Corporation (West Palm Beach, FL) for furnishing the commercial cpTi samples.

References

1. B. D. Ratner, D. G. Castner, T. A. Horbett, T. J. Lenk, K. B. Lewis, and R. J. Rapoza, "Biomolecules and surfaces," *J. Vac. Sci.*, **A8**, 2306–2317 (1990).
2. D. M. Brunette, "Interactions of epithelial cells with foreign surfaces," *CRC Crit. Rev. Biocompat.*, **1**, 323–370 (1986).
3. B. Kasemo and J. Lausmaa, "Surface science aspects on inorganic biomaterials," *CRC Crit. Rev. Biocompat.*, **2**, 335–380 (1986).
4. A. G. Brownell, C. C. Bessem, and H. C. Slavkin, "Possible function of mesenchyme cell-derived fibronectin during formation of basal lamina," *Proc. Natl. Acad. Sci. USA*, **78**, 3711–3715 (1981).
5. C.A. Lewis, R. M. Pratt, J. P. Pennypacker, and J. R. Hassell, "Inhibition of limb chondrogenesis *in vitro* by vitamin A: Alteration in cell surface characteristics," *Dev. Biol.*, **64**, 31–47 (1978).
6. W. Dessau, J. Sasse, R. Timpl, F. Jilek, and K. von der Mark, "Synthesis and extracellular deposition of fibronectin in chondrocyte cultures," *J. Cell Biol.*, **79**, 342–355 (1978).
7. R. M. Pratt and K. M. Yamada, "Enhanced cellular fibronectin accumulation in chondrocytes treated with vitamin A," *Cell*, **17**, 821–826 (1979).
8. R. A. Proctor, "Fibronectin: A brief overview of its structure, function, and physiology," *Rev. Infect. Dis.*, **9**, S317–S321 (1987).
9. F. Grinnell and M. K. Feld, "Fibronectin adsorption on hydrophilic and hydrophobic surfaces detected by antibody binding and analyzed during cell adhesion in serum containing solution," *J. Biol. Chem.*, **257**, 4888–4893 (1982).
10. D. D. McAbee and F. Grinnell, "Fibronectin mediated binding and phagocytosis of polystyrene latex beads by baby hamster kidney cells," *J. Cell Biol.*, **97**, 1515–1523 (1983).
11. C. E. Wolff and C.-S. Lai, "Fluorescence energy transfer detects changes in fibronectin structure upon surface binding," *Arch. Biochem. Biophys.*, **268**, 536–545 (1989).
12. C. E. Wolff and C.-S. Lai, "Inter-sulphydryl distances in plasma fibronectin determined by fluorescence energy transfer: Effect of environmental factors," *Biochemistry*, **29**, 3354–3361 (1990).
13. S.-S. Cheng, K. K. Chittur, C. N. Sukenik, L A. Culp, and K. Lewandowska, "The conformation of fibronectin on self-assembled monolayers with different surface composition: an FTIR/ATR study," *J. Colloid Interface Sci.*, **162**, 135–143 (1994).
14. R. W. Watkin and C. R. Robertson, "A total internal-reflection technique for the examination of protein adsorption," *J. Biomed. Mater. Res.*, **11**, 915–938 (1977).
15. R. Emch, X. Clivaz, C. Taylor-Denes, P. Vaudaux, P. Descouts, "Scanning tunneling microscopy for studying the biomaterial–biological tissue interface," *J. Vac. Sci. Technol.*, **A8**, 655–658 (1990).
16. R. Emch, F. Zenhausern, M. Jobin, M. Taborelli, and P. Descouts, "Morphological difference between fibronectin sprayed on mica and on PMMA," *Ultramicroscopy*, **42–44**, 1155–1160 (1992).
17. G. Binnig, C. F. Quate, and C. Gerber, "Atomic force microscope," *Phys. Rev. Lett.*, **56**, 930–933 (1986).
18. C. Wyman, E. Grotkopp, C. Bustamante, H. C. M. Nelson, "Determination of heatshock transcription factor 2 stoichiometry at looped DNA complexes using scanning force microscopy," *EMBO J.*, **14**, 117–123 (1995).
19. R. O. Hynes, *Fibronectins*, Springer Series in Molecular Biology, A. Rich (ed.), Springer–Verlag, New York, 1990, pp. 200–364.
20. N. R. Armstrong and R. K. Quinn, "Auger and X-ray photoelectron spectroscopic and electrochemical characterization of titanium thin film electrodes," *Surf. Sci.*, **67**, 451–468 (1977).
21. K. E. Healy and P. Ducheyne, "Oxidation kinetics of titanium films in model physiologic environments," *J. Colloid Interface Sci.*, **150**, 404–417 (1992).
22. K. E. Healy and P. Ducheyne, "Hydration and preferential molecular adsorption on titanium *in vitro*," *Biomaterials*, **13**, 553–561 (1992).
23. K. E. Dombrowski, S. E. Wright, J. C. Birkbeck, and W. E. Moddeman, "X-ray photoelectron spectroscopy of amino acids, polypeptides and simple carbohydrates," in *Methods in Protein Surface Analysis*, M. Z. Atassi and E. Appella (eds.), Plenum Press, New York, 1995, pp. 251–260.
24. P. A. Gerin, P. B. Dengis, and P. G. Rouxhet, "Performance of XPS analysis of model biochemical compounds," *J. Chim. Phys.*, **92**, 1043–1065 (1995).
25. R. E. Baier, R. C. Dutton, and V. L. Gott, in *Surface Chemistry of Biological Systems*, Plenum Press, New York, 1970, pp. 235–260.
26. J. F. Oliver, C. Huh, and S. G. Mason, "An experimental study

of some effects of solid surface roughness on wetting," *Coll. Surfaces*, **1**, 79–104 (1980).

27. R. D. Kulkarni and P. Somasundaran, "Mineralogical heterogeneity of ore particles and its effects on the interfacial characteristics," *Powder Tech.*, **14**, 279–285 (1976).
28. I. J. Lin and P. Somasundaran, "Alterations in properties of samples during their preparation by grinding," *Powder Tech.*, **6**, 171–180 (1972).
29. D. V. Kilpadi and J. E. Lemons, "Surface energy characterization of unalloyed titanium implants," *J. Biomed. Mater. Res.*, **28**, 1419–1425 (1994).
30. Y. Oshida, R. Sachdeva, and S. Miyazaki, "Changes in contact angles as a function of time on some pre-oxidized biomaterials," *J. Mater. Sci. Mater. Med.*, **3**, 306–312 (1992).
31. Y. Oshida, R. Sachdeva, S. Miyazaki, and J. Daly, "Effects of shot-penning on surface contact angles of biomaterials," *J. Mater. Sci. Mater. Med.*, **4**, 443–447 (1993).
32. P. Ducheyne, "Titanium and calcium phosphate ceramic dental implants, surface, coatings, and interfaces," *Oral Implantol.*, **14**, 325–340 (1988).
33. A. Wisbey, P. J. Gregson, L. M. Peter, and M. Tuke, "Effect of surface treatment on the dissolution of titanium-based implant materials," *Biomaterials*, **12**, 470–473 (1991).
34. D. Kawahara, Y. Kimura, M. Nakamura, and H. Kawahara, "Studies on the tissue adhesive capability to titanium by dynamic wettability test and cell attachment, *in vitro*," *Clin. Mater.*, **14**, 229–233 (1993).
35. C. M. Demanet, S. Shrivastava, and J. P. F. Sellschop, "Scanning force microscopy analysis of the surface of ion-irradiated diamond," *Surf. Interface Anal.*, **23**, 115–119 (1995).
36. V. E. Koteliansky, M. V. Bejanian, and V. N. Smirnov, "Electron microscopy study of fibronectin structure," *FEBS Lett.*, **120**, 283–286 (1980).
37. V. E. Koteliansky, M. A. Glukhova, M. V. Bejanian, V. N. Smirnov, V. V. Filimonov, O. M. Zalite, and S. Y. Venyaminov, "A study of the structure of fibronectin," *Eur. J. Biochem.*, **119**, 619–624, (1981).
38. J. Engle, E. Odermatt, A. Engel, J. A. Madri, H. Furthmayr, H. Rohde, and R. Timpl, "Shapes, domain organizations and flexibility of laminin and fibronectin, two multifunctional proteins of the extracellular matrix," *J. Mol. Biol.*, **150**, 97–120 (1981).
39. H. P. Erickson, N. Carrell, and J. McDonagh, "Fibronectin molecule visualized in electron microscopy: A long, thin, flexible strand," *J. Cell. Biol.*, **91**, 673–678 (1981).
40. E. G. Williams, P. A. Janmey, J. D. Ferry, and D. F. Mosher, "Conformational states of fibronectin: Effects of pH, ionic strength, and collagen binding," *J. Biol. Chem.*, **257**, 14973–14978 (1982).
41. E. Odematt and J. Engel, "Physical properties of fibronectin," in *Fibronectin, Biology of Extracellular Matrix*, D. F. Mosher (ed.), Academic Press, Inc., New York, 1989, pp. 25–45.
42. B. Sjöberg, M. Eriksson, E. Österlund, S. Pap, and K. Österlund, "Solution structure of human plasma fibronectin as a function of NaCl concentration determined by small-angle neutron diffraction," *Eur. J. Biophys.*, **17**, 5–11 (1989).
43. M. J. Benecky, C. G. Kolvenbach, R. W. Wine, J. P. DiOrio, and M. W. Mosesson, "Human plasma fibronectin structure probed by steady-state fluorescence polarization: Evidence for a rigid oblate structure," *Biochemistry*, **29**, 3082–3091 (1990).
44. M. Y. Khan, M. S. Medow, and S. A. Newman, "Unfolding transitions of fibronectin and its domains, stabilization and structural alternation of the N-terminal domain by heparin," *Biochem. J.*, **270**, 33–38 (1990).
45. M. J. Benecky, R. W. Wine, C. G. Kolvenbach, and M. W. Mosesson, "Ionic-strength- and pH-dependent conformational states of human plasma fibronectin," *Biochemistry*, **30**, 4298–4306 (1991).
46. E. Österlund, "The secondary structure of human plasma fibronectin: Conformational changes induced by acidic pH and elevated temperatures; a circular dichroic study," *Biochim. Biophys. Acta*, **955**, 330–336 (1988).
47. M. Rocco, E. Infusini, M. G. Daga, L. Gogioso, and C. Cuniberti, "Models of fibronectin," *EMBO J.*, **6**, 2343–2349 (1987).
48. C.-S. Lai and N. M. Tooney, "Electron spin resonance spin label studies of plasma fibronectin: Effect of temperature," *Arch. Biochem. Biophys.*, **228**, 465–473 (1984).
49. S. S. Alexander, Jr., G. Colonna, and H. Edelhoch, "The structure and stability of human plasma cold-insoluble globulin," *J. Biol. Chem.*, **254**, 1501–1505 (1979).
50. C. Wolff and C.-S. Lai, "Fluorescence energy transfer detects changes in fibronectin structure upon surface binding," *Arch. Biochem. Biophys.*, **268**, 536–545 (1989).
51. H. P. Erickson and N. A. Carrell, "Fibronectin in extended and compact conformations," *J. Biol. Chem.*, **258**, 14539–14544 (1983).
52. G. K. Iwamoto, L. C. Winterton, R. S. Stoker, R. A. van Wagenen, J. D. Andrade, and D. F. Mosher, "Fibronectin adsorption detected by interfacial fluorescence," *J. Colloid Interface Sci.*, **106**, 459–464 (1985).
53. C. Narasimhan, C.-S. Lai, A. Haas, and J. McCarthy, "One free sulfhydryl group of plasma fibronectin becomes titratable upon binding of the protein to solid substrates," *Biochemistry*, **27**, 4970–4973 (1988).
54. C. Narasimhan and C.-S. Lai, "Conformational changes of plasma fibronectin detected upon adsorption to solid substrates: A spin-labeled study," *Biochemistry*, **28**, 5041–5046 (1989).
55. D. F. Mosher, "Physiology of fibronectin," *Ann. Rev. Med.*, **35**, 561–575 (1984).
56. V. Vogel, "Fibronectin in surface-adsorbed state," in *Proteins at Interfaces. II. Fundamentals and Applications*, T. A. Herbett and J. L. Brash (eds.), American Chemical Society, Washington DC, 1995, pp. 505–518.
57. J. A. McDonald, B. J. Quade, T. J. Broekelmann, R. LaChance, K. Forsman, E. Hasegawa, and S. Akiyama, "Fibronectin cell-adhesive domain and an amino-terminal matrix assembly domain participate in its assembly into fibroblast," *J. Biol. Chem.*, **262**, 2957–2967 (1987).
58. J. Sottile, J. Schwarzbauer, J. Selegue, and D. F. Mosher, "Five type I modules of fibronectin form a functional unit that binds to fibroblasts and *Staphylococcus aureus*," *J. Biol. Chem.*, **266**, 12840–12843 (1991).
59. J. E. Schwarzbauer, "Identification of fibronectin sequences required for assembly of a fibrillar matrix," *J. Cell. Biol.*, **113**, 1463–1473 (1991).
60. A. Morla and E. Ruoslahti, "A fibronectin self-assembly site involved in fibronectin matrix assembly: Reconstruction in a synthetic peptide," *J. Cell Biol.*, **118**, 421–429 (1992).
61. D. F. Mosher and R. B. Johnson, "*In vitro* formation of disulfide-bonded fibronectin multimers," *J. Biol. Chem.*, **258**, 6595–6601 (1983).
62. D. F. Mosher, F. J. Fogerty, M. A. Chernousov, and E. L. R. Barry, "Assembly of fibronectin into extracellular matrix," *Ann. NY Acad. Sci.*, **614**, 167–180 (1991).